Despeckling the 2D Medical Ultrasound Image through Individual Despeckling of the Envelopes of Its 1D Radio Frequency Echo Lines by STFT

Jawad F. Al-Asad
Electrical Engineering, Prince Mohammad Bin Fahd University, Khobar, KSA
Email: jalasad@pmu.edu.sa

***Abstract*—In this paper Short Time Fourier Transform (STFT) is used to despeckle the medical ultrasound image before reconstruction. STFT is applied individually to the one dimensional (1D) Radio Frequency (RF) envelopes that constitute the two dimensional (2D) image. Total Variation Filter (TVF) and Anisotropic Diffusion Filter (ADF) are also applied to the speckle noisy 2D ultrasound image after reconstruction. Performance comparison is held between despeckling the ultrasound image before reconstruction and after reconstruction. Despeckling the ultrasound image before reconstruction through STFT has removed the speckle noise more efficiently than TVF and ADF. It also maintained the texture of the original image and that is compared to STFT performance when applied to the 2D image after reconstruction. TVF is found more efficient in removing speckle when applied through overlapping blocks compared with applying it as a whole to the 2D image. ADF is found outperforming TVF in removing speckle noise and it is found more efficient when applied as a whole to the 2D image compared with applying it through overlapping blocks.**

***Index Terms*—ultrasound image, RF envelope, down-sampling, STFT, speckle noise**

I. Introduction

Ultrasound medical imaging is a real time imaging modality that is cost effective and harmless to the human body. Unlike other medical imaging modalities, the quality of the image of this modality is degraded by the speckle noise.

Most despeckling schemes found in literature have removed speckle noise from the medical ultrasound image as it appears on the screen. A fundamental stage in the ultrasound machine is beam-forming [1]. Beam-forming refers to the process by which the signals on separate channels, each received from a different transducer element, are combined to form a single RF (Radio frequency) signal representative of the echoes received from the tissues by the defined transducer aperture. Envelope detection of each RF_line is either done by Hilbert transform [2] or by In-phase Quadrature IQ demodulation [3]. The envelopes of RF_lines are lined up side by side to form the envelope image, and then subjected to down-sampling (decimation) which results in correct spatial aspect ratio.

The multiplicative nature of the speckle noise formation was used in [4] in which the author proposes to convert the multiplicative speckle noise into an additive noise by applying the logarithmic transformation to a speckle-noisy image. Subsequently, Wiener filtering is used in order to reject the resultant additive noise, followed by the exponential transformation. General speckle noise reduction methods found in literature are based on averaging filters and adaptive weighted median filters [5] which can effectively suppress speckle noise, however, they fail to preserve many useful details. It has been reported in [6] that the log transformed multiplicative noise is spiky in nature and follows Fisher-Tippett distribution. The authors have proposed a preprocessing outlier shrinkage stage to Gaussianize the log transformed noise prior to de-noising. It was shown that HWDS does not improve the Signal-to-Noise Ratio (SNR) [7] because the wavelet transformed speckle coefficients are larger than the threshold value, thus not suitable for removing the speckle noise in ultrasound images. In [8] Karhunen-Loeve (K-L) transform -also known as PCA- is used in the wavelet packet domain to denoise AWGN where few principle components are assumed to represent the signal while noise is assumed to spread over all the transformed coefficients. A shrinkage function is then applied on the transformed coefficients to remove noise. In [9], [10] Total Variation filtering and Anisotropic Diffusion filtering were found less efficient than PCA in removing speckle noise from the medical ultrasound image. HWDS was also found the most sensitive to outliers resulted from the log transformation of the multiplicative noise. The principle of overlapping blocks and a comparative performance study of different transforms to remove the speckle noise from medical ultrasound images was investigated in [11], [12].

A review for some of the most important methods for ultrasound image enhancement was made in [13]. Techniques were classified into two groups: preprocessing and post-processing. Preprocessing techniques attempt to shape the ultrasound field to compensate for known degradations due to tissue properties. They consist of modifications in the signal generation and/or acquisition stages. Post-processing, on

Manuscript received April 10, 2016; revised August 12, 2016.

doi: 10.18178/joig.4.2.67-72

the other hand is confined in speckle reduction methods applied to the speckle noisy image as it appears on the screen. In [14] speckle reduction in ultrasound images is achieved by frequency compounding. A general scheme for ultrasound image processing based on the notion of sup resolution technique that combines multiple low resolution images of the same scene to produce one high resolution image. The main drawback of this method is that it requires multiple images for the same region of interest to produce high resolution image with less speckle.

For non-stationary and non-Gaussian processes, time-frequency analysis methods appear to provide the necessary analysis to the time varying properties of signals. Non-stationary processes contain signals that have a noticeably different spectrum in time. Short-Time Fourier Transform (STFT) representation [15] shows itself as a suitable tool for the sake of noise removal from a non-stationary signal.

In this paper, STFT, TVF [16] and ADF [17] are applied to the 2D ultrasound envelope image after reconstruction. STFT and TVF were applied through overlapping blocks of q x p size, while ADF is applied in full to the 2D image. STFT* is then applied through overlapping segments of q x 1 size to the envelope of each RF line before reconstruction followed by its application to the lateral dimension of the 2D image after reconstruction as shown in Fig. 1. STFT* indicates that the despeckling procedure is different from STFT in that it is applied to the envelopes of each RF line rather than applied to the final 2D image size. A performance comparison is held among the four despeckling procedures when applied to the speckle noisy ultrasound envelope image before and after reconstruction.

This paper is organized as follows: Section II presents the adopted signal model and the methods to filter out the speckle noise. Section III summarizes the experimental results of the methods when applied to a simulated image and to a real ultrasound image. The paper is concluded in Section IV.

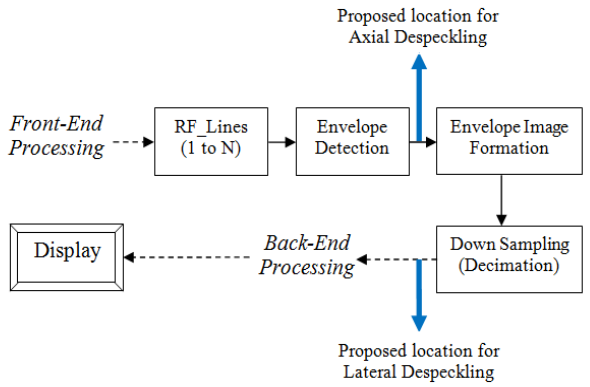

Figure 1. Proposed locations of depeckling in B-mode imaging.

II. Ultrasound Signal Model and the Procedures of Despeckling

A generalized model of a speckled image as proposed in [4] is given by:

$$g(n,m) = f(n,m)u(n,m) + \xi(n,m) \tag{1}$$

where g, f, u and ξ stand for the observed envelope image original image, multiplicative and additive components of the speckle noise, respectively. Here the indices n and m denote the axial and lateral indices of the image samples (or, alternatively, the angular and range indices for sector images).

The model in (1) has been successfully used both in ultrasound and SAR imaging. When applied to ultrasound images, model (1) can be considerably simplified by disregarding the additive noise term. This leads to the following simplified model:

$$g(n,m) \approx f(n,m)u(n,m) \tag{2}$$

An alternative model proposed in [5] describes the speckle noise as an additive noise, whose amplitude is proportional to the square root of the true image. However, this model was proposed to account for the speckle pattern, as it appears on “screen”, rather than the envelope detected echo signal. Consequently, adopting the model in (2) as the basic model, it is assumed that the image $g(n,m)$ is observed before the system processing is applied [6].

Implementation of STFT indicates that frequency information is localized for each window and is otherwise independent of the behavior of the signal at other times. In discrete form the STFT is expressed as:

$$S(n,k) = \sum_{m=-L}^{L} x(m)w(n-m)e^{-j2\pi km/N},\ k = 0,1\ldots N-1 \tag{3}$$

where $S(n,k)$ is the frequency over k shifts. The $w(n-m)$ is the window shift of zero value outside a short finite interval and $x(m)$ is the original signal in time domain.

After log transformation, TVF and STFT are applied through small blocks of q x p size. TVF is applied with suitable number of iterations and a regularization smoothing parameter [16]. The largest magnitude coefficient of the STFT time-frequency plane per each block size is selected for reconstruction through inverse STFT while rest of coefficients are hard thresholded to zeros. TVF and STFT are found more efficient when applied through overlapping blocks rather than applying them in full to the 2D image. The despeckled image in either STFT approach, STFT* approach or TVF approach is reconstructed by adding up all the updates for all overlapping blocks and then each sample is averaged by the number of updates. ADF filter is found more efficient when applied in full rather than in overlapping blocks to the log transformed image using suitable parameters of number of iterations, conduction coefficient, speed of diffusion and region size (narrow or wide) [17].

To assess the denoising capabilities, five image quality measures are used: the resolution parameter α, the edge detection parameter β, signal to noise ratio SNR, speckle signal to noise ratio S-SNR and peak signal to noise ratio PSNR. The SNR, S-SNR, and PSNR can be reported in dB unit by taking 10 $\log_{10}$(.) of their values [10].

III. RESULTS

A. In Silico Expirement

To simulate speckle noise appearance on the screen an MRI map image for the abdomen was subjected to linear scanning through the “Field II Program” [18]. The image in Fig. 2-a consists of 256 A_scans penetrating 4096 scatterers per cm^2 with a lateral resolution of 0.156mm. This number of scatterers is chosen in accordance with the simulations made in [19]. The envelopes of the RF echo signals are obtained by taking the absolute value of the Hilbert transformation of the RF echo signals [19]. All of the envelopes are rearranged side-by-side to form a 2D envelope image. The image is down-sampled from 4096x256 to yield 256x256 image size shown in Fig. 2-a. The corresponding speckle noisy version, shown in Fig. 2-b, is created by corrupting the undecimated envelope image by noise according to (2).

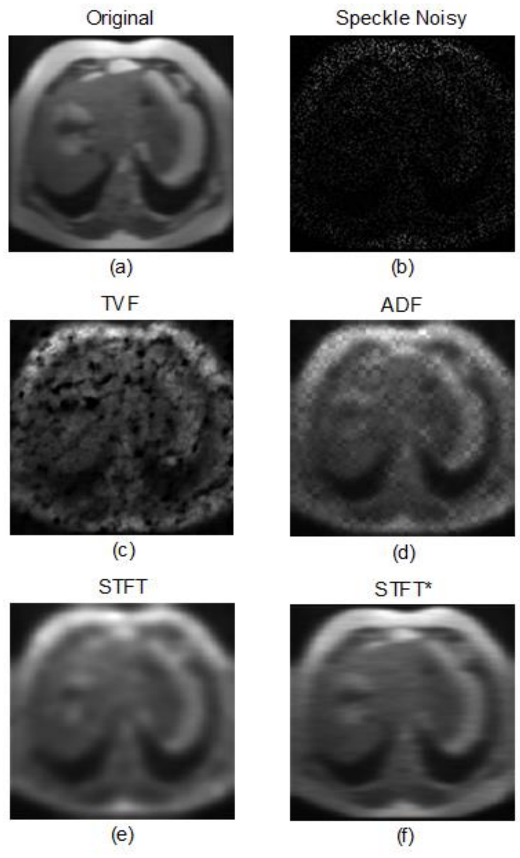

Figure 2. Despeckling schemes applied to the 256x256 image size. STFT* is applied to the envelopes of the 4096 long RF lines individually.

STFT and TVF are applied with block size of 16x16 to the 256x256 image size shown in Fig. 2-b. A dyadic block size is chosen in accordance to our findings in [10] where 16 is the square root of 256. TVF is applied with a smoothing parameter of 400 and 100 iterations. ADF is applied in full to the 2D image with 30 iterations, conduction coefficient of 30, speed of diffusion of 0.25 and favoring wide regions. The numerical performance is listed in Table I as an average of 10 independent trials. STFT* is applied to the RF envelopes with 64 (square root of 4096) sized 1D segments, and then applied to the lateral dimension of the 2D image after down-sampling with 16 sized segments.

It is clearly noticed either from the numerical performance in Table I or from the visual performance in Fig. 2 that ADF has outperformed TVF in all parameters including the resolution (α) where less α indicates better resolution. STFT has outperformed ADF and TVF in terms of S-SNR, SNR and PSNR. However, this performance was on the account of edge detection (β) and resolution (α) where TVF and ADF performed better. When STFT* is applied to the envelopes of each RF line before reconstructing the 2D image, followed by its application laterally to the 2D image after down-sampling, its performance has outperformed the other despeckling schemes and procedures. SNR, PSNR and β have improved dramatically. Resolution has improved as well and can be noticed visually by comparing Fig. 2-f to Fig. 2-e or by noting the reduction of α parameter from 0.101 down to 0.095 in Table I.

It is important to notice that this improvement of performance is accompanied by a reduction in S-SNR from 1.72 for STFT down to 1.52 for STFT*. We will use this hint for the conclusion part in the In Vivo experiment where reduction in S-SNR is swapped by great improvement in terms of SNR, PSNR, β and α.

TABLE I. NUMERICAL PERFORMANCE OF DESPECKLING SCHEMES APPLIED TO THE IMAGE IN FIG. 2-B

	S-SNR Ratio	SNR dB	PSNR dB	β	α
TVF	1.10	9.05	17.62	0.077	0.012
ADF	1.50	13.85	21.82	0.068	0.011
STFT	1.72	16.25	23.68	0.018	0.101
STFT*	1.52	23.47	28.55	0.381	0.095

Fig. 3 displays the axial and lateral profiles of the images in Fig. 2. By comparing the axial and lateral profiles of STFT in Fig. 3-e respectively with those in Fig. 3-c for TVF and with those in Fig. 3-d for ADF, we can notice the superiority of STFT in removing the speckle noise. The original texture of the image can be further preserved if STFT denoted by STFT* in Fig. 3-f is applied to the envelope of each RF line individually before reconstructing the image. The despeckled axial and lateral profiles through STFT* in Fig. 3-f respectively, almost fit to the original (noise free) profiles indicated by the dotted lines.

Fig. 4 displays the percentile improvement of despeckling the image before reconstruction versus after reconstruction through STFT. Despeckling the image before reconstruction over despeckling it after reconstruction has maintained around 0.45 % improvement in SNR, 0.2% improvement in PSNR and over 20% improvement in β. α is improved by around 0.05%. The reduction of around 0.12% in S-SNR has contributed towards a better resolution as well.

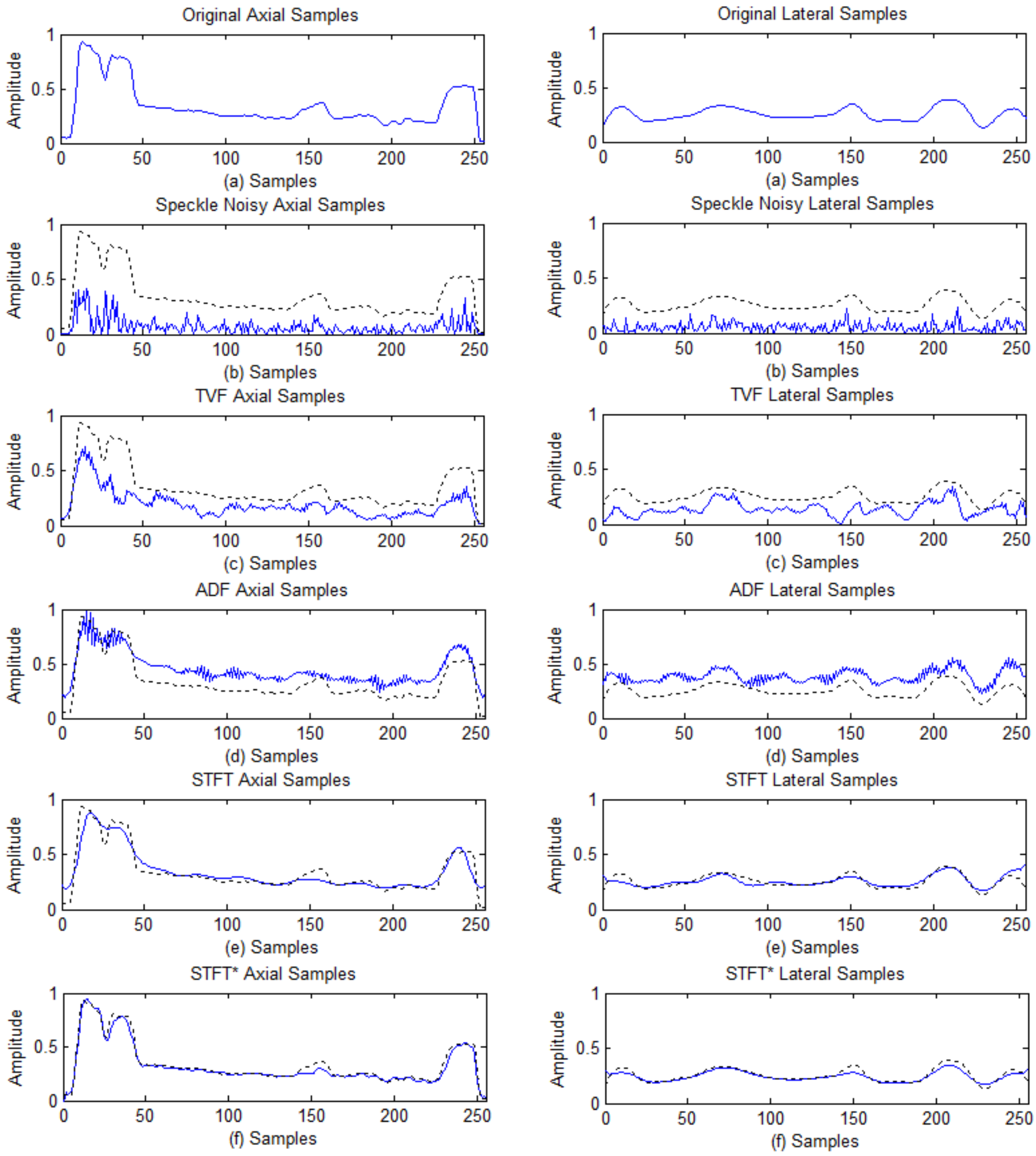

Figure 3. Middle axial and lateral profiles corresponding to the images in Fig. 2. The dotted line in the plots b through f is the original (noise free) axial and lateral profiles in a, and used for convenient visual comparison.

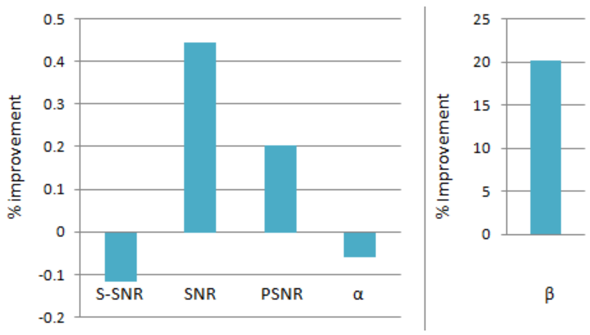

Figure 4. Percentile improvements of despeckling 4096x256 size over despeckling 256x256 final image size. Note that negative percentage of Alpha indicates better resolution.

B. In Vivo Expirement

Real RF data is downloaded for a patient diagnosed with Fibroadenoma [20]. 1024 long RF ultrasound echo lines are lined up and then decimated to form the 256x256 image size shown in Fig. 5-a. For despeckling performance analysis the image is chosen to show the cyst appearing in the middle. STFT and TVF are applied with block size of 16 x16 to the 256x256 image size shown in Fig. 5-a. TVF is applied with a smoothing parameter of 450 and 200 iterations. ADF is applied in full to the 2D image with 30 iterations, conduction coefficient of 30, speed of diffusion of 0.25 and favoring wide regions. The numerical performance is listed in Table II. STFT* is applied to the RF envelopes with 32 (square root of 1024) sized 1D segments, and then applied to the lateral dimension of the 2D image after down-sampling with 16 sized segments.

Similar to the findings in the In Silico experiment, Table II shows that STFT has numerically outperformed TVF and ADF in terms of S-SNR. TVF provided the best resolution compared with the other despeckling procedures but that was on the account of speckle removal efficiency. The reduction of S-SNR and α for

STFT* compared to STFT in Table II is seen in Table I for the In Silico experiment. However, this reduction in Table II is a means to expect better SNR, PSNR and β as can be inferred by comparing Fig. 5-e with Fig. 5-d, or by comparing Fig. 5-e with Fig. 5-b or c (for TVF and ADF respectively).

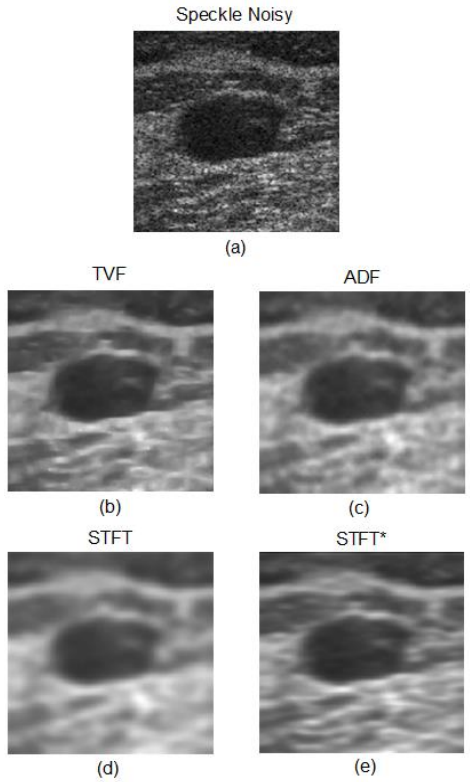

Figure 5. Despeckling schemes applied to the 256x256 image size. STFT* is applied to the envelopes of the 1024 long RF lines individually.

TABLE II. NUMERICAL PERFORMANCE OF DESPECKLING SCHEMES APPLIED TO THE IMAGE IN FIG. 5-A

	TVF	ADF	STFT	STFT*
S-SNR	1.476	1.549	1.658	1.482
α	0.057	0.070	0.077	0.062

Such a result tells us that it is not enough to devise an efficient despeckling scheme, but it is also important to find the proper location of applying it in ultrasound imaging.

IV. CONCLUSION

Speckle noise removal before ultrasound image reconstruction is investigated in this paper and compared with speckle noise removal after reconstruction. STFT, ADF and TVF schemes are investigated in removing speckle noise when applied to the envelope image after reconstruction. ADF is found more efficient in removing speckle noise when applied in full to the 2D image, while TVF is found more efficient in removing speckle noise when applied through small dyadic overlapping blocks. STFT has outperformed ADF and TVF in terms of S-SNR, SNR and PSNR, however that was on the account of edge detection and resolution. The performance of STFT is dramatically improved over the other despeckling procedures when applied in the proper location in B-mode scanning and that is on each of the 1D envelopes of the RF echoes and then on each 1D lateral dimension of the 2D image after decimation. Chirplet transform should be tested against STFT in the future.

REFERENCES

[1] E. Brunner, "Ultrasound system consideration and their impact on front-end components," Analog Devices, Inc., 2002.

[2] S. C. Kak, "Discrete hilbert transform," *Proceedings of the IEEE*, vol. 58, no. 4, pp. 585–586, April 1970.

[3] J. Kirkhorn, "Introduction to IQ-demodulation of RF-data," Technical report, IFBT, NTNU, 1999.

[4] A. K. Jain, *Fundamental of Digital Image Processing*, Englewood Cliffs, NJ: Prentice-Hall, 1989.

[5] T. Loupas, W. N. Mcdicken, and P. L. Allan, "An adaptive weighted median filter for speckle suppression in medical ultrasonic images," *IEEE Trans. Circuits Syst*., vol. 36, pp. 129–135, Jan. 1989.

[6] O. V. Michailovich and A. Tannenbaum, "Despeckling of medical ultrasound images," *IEEE Trans. Ultrasonics, Ferroelectrics, and Frequency Control*, vol. 53, no. 1, pp. 64-78, January 2006.

[7] E. Nadernejad, "Despeckle filtering in medical ultrasound imaging," *Contemp. Eng. Sci*., vol. 2, no. 1, pp. 17–36, 2009.

[8] B. K. Sahu and P. D. Sawami, "Image denoising using principal component analysis in wavelet domain and total variation regularization in spatial domain," *International Journal of Computer Applications*, vol. 71, no. 12, May 2013.

[9] J. F. Al-Asad, A. Moghadamjoo, and L. Ying, "Ultrasound image de-noising through K-L transform with overlapping segments," in *Proc. IEEE International Symposium on Biomedical Imaging: From Nano to Macro*, Boston, USA, June 2009.

[10] J. F. Al-Asad, A. Moghadamjoo, and U. Techavipoo, "An ultrasound image despeckling approach based on principle component analysis," *International Journal of Image Processing*, vol. 8, no. 4, pp. 156–177, July 2014.

[11] J. F. Al-Asad, "Transform domain based approach for medical ultrasound image de-speckling through overlapping blocks," in *Proc. IASTED International Conference on Computational Bioscience*, Cambridge, United Kingdom, July 2011.

[12] J. F. Al-Asad and A. Moghadamjoo, "Short-time Fourier transform and Wigner-Ville transform for ultrasound image de-noising through dynamic mask thresholding," in *Proc. IEEE International Conference on Bioinformatics and Biomedical Engineering*, Chengdu, China, June 2010.

[13] S. H. C. Ortiz, T. Chiu, and M. D. Fox, "Ultrasound image enhancement: A review," *Biomedical Signal Processing and Control*, vol. 7, no. 5, pp. 419–428, September 2012.

[14] M. Tsakalakis and N. G. Bourbakis, "Ultrasound image despeckling/denoising based on a novel multi-transducer architecture," in *Proc. IEEE International Conference on Bioinformatics and Bioengineering*, Nov. 2014, pp. 62–68.

[15] W. Yuegang J. Shao, and X. Hongtao, "Non-stationary signals processing based on STFT," in *Proc. Eighth International Conference on Electronic Measurement and Instruments*, 2007.

[16] L. Rudin, S. Osher, and E. Fatemi, "Nonlinear total variation based noise removal algorithms," *Phys. D*, vol. 60, pp. 259–268, 1992.

[17] P. Perona and J. Malik. "Scale-space and edge detection using anisotropic diffusion," *IEEE Trans. on Pattern Analysis and Machine Intelligence*, vol. 12, no. 7, pp. 629-639, July 1990.

[18] J. A. Jensen, "Field: A program for simulating ultrasound systems," *Medical & Biological Engineering & Computing*, vol. 34, pp. 351–353, 1996.

[19] G. Georgiou and F. S. Cohen, "Statistical characterization of diffuse scattering in ultrasound images," *IEEE Trans. Ultrason. Ferroelectr. Freq. Control*, vol. 45, no. 1, pp. 57–64, Jan. 1998.

[20] Patient echo data from Siemens Antares™ ultrasound system. [Online]. Available: http://ultrasonics.bioengineering.illinois.edu/data_patient.asp

Jawad F. Al-Asad is currently an Assistant Professor in the Electrical Engineering department at Prince Mohammad Bin Fahd University/Kingdom of Saudi Arabia. He earned his PhD in Electrical Engineering from the University of Wisconsin-Milwaukee, USA in 2009, his Master degree in Electrical Engineering from the University of Jordan, Jordan in 1999 and his Bachelor degree in Electrical Engineering from the University of Engineering and Technology, Pakistan in 1994. After he earned his PhD he joined DeVry University-Chicago/USA as a senior professor teaching in the biomedical, electrical and computer engineering technology majors. His current research interests are in biomedical signal and image processing and reconstruction.